



# The kinetics of formation and growth of TiC precipitates in Ti-modified stainless steel studied by positron annihilation spectroscopy

Padma Gopalan <sup>a,\*</sup>, R. Rajaraman <sup>a</sup>, B. Viswanathan <sup>a</sup>, K.P. Gopinathan <sup>b</sup>,  
S. Venkadesan <sup>c</sup>

<sup>a</sup> *Materials Science Division, Indira Gandhi Centre for Atomic Research, Kalpakkam-603 102, India*

<sup>b</sup> *Department of Physics, Cochin University of Science and Technology, Kochi-682 022, India*

<sup>c</sup> *Materials Development Division, Indira Gandhi Centre for Atomic Research, Kalpakkam-603 102, India*

Received 2 September 1997; accepted 5 March 1998

---

## Abstract

The formation and growth of TiC precipitates in Ti-modified austenitic stainless steel (D-9 alloy) is monitored by positron lifetime spectroscopy. From isochronal annealing studies various recovery stages are identified. TiC precipitates are found to be more stable in 20% cold worked alloy than in a 17.5% cold worked sample. From the isothermal annealing studies, it is found that TiC precipitation is controlled by dislocations. The limited temperature dependence of dislocation controlled TiC precipitation is governed by an apparent activation energy of 1.6 eV. In 20% cold worked alloy, TiC precipitates are found to be stable against growth even after 1000 h of annealing at 923 K. For higher annealing temperatures, TiC precipitate coarsening occurs due to recrystallisation. © 1998 Elsevier Science B.V. All rights reserved.

---

## 1. Introduction

Austenitic stainless steels have been adopted as candidate materials for the fast breeder reactor core applications. Many efforts at improving their strength at elevated temperature and swelling resistance have been made to prolong their lives. In order to improve and enhance their resistance to irradiation induced void swelling, efficient traps for vacancies and helium such as dislocations and precipitate–matrix interfaces have been introduced by adjusting alloying elements and thermo-mechanical treatments [1,2]. Accordingly, Ti-modified austenitic stainless steel has become a primary candidate material for structural applications, with extensive studies on this alloy reported in recent years, covering different physical and mechanical properties (see Refs. [1–6] and references contained therein). Ti-modified stainless

steel type D-9 with Ti/C ratio of 6 is the material chosen to be used for the fuel clad and the hexagonal wrapper for the fuel sub-assemblies of prototype fast breeder reactors in India [3]. Studies on D-9 alloy using microhardness measurements [3] showed that 17.5% is the highest prior cold work level that gives minimum variation in hardness measurements, and a refined analysis of hardness measurements in D-9 alloy concludes that 20% cold working is the optimum level for the stability of this alloy [6]. This is important because the production of cold-work-induced microstructures, which are stable at service temperatures up to 973 K in the reactor, is one of the crucial controlling factors for irradiation induced void swelling [3]. It has also been reported that the beneficial effects of prior cold work are lost in type 316 stainless steel by heating to 923 K for 100 h prior to irradiation [7,8]. Hence, the optimisation of the cold worked level and the stability of the induced microstructure are very important.

The clad wrapper would be subjected to prolonged exposure at an elevated service temperature of about

---

\* Corresponding author. Fax: +91-44114 40381; e-mail: gpadma@igcar.ernet.in.

823 K and also to short time transient to higher temperatures. For prototype fast breeder reactor clad, the specified maximum mid-wall hot spot temperature is 973 K in the steady state and 1073 K in the transient state [3]. Studies on the microstructural evolution of the material due to aging at elevated temperature are important because the latter would lead to alteration in the microstructure and growth of TiC precipitates.

Positron annihilation spectroscopy (PAS) is an established technique for studies on the properties of vacancies and dislocations [9] as well as studies on early stages of solute atom clustering and precipitation [10]. Positron annihilation results showing significant refinement of helium bubble size and bubble concentration upon titanium addition have been reported in Ti-stabilised austenitic stainless steel [11]. In our recent report, we have demonstrated the ability of PAS to monitor the TiC precipitation process in D-9 alloy [12]. In this paper, results of studies on the kinetics of the formation and growth of TiC precipitates by positron annihilation spectroscopy are discussed.

## 2. Experimental details

The chemical composition of D-9 alloy used in the present study is given elsewhere [12]. D-9 samples of dimensions 10 mm × 10 mm × 0.5 mm were subjected to solution annealing treatment at 1343 K for 30 min, followed by holding at 1373 K for 5 min [13] and then slow cooling. These samples were cold rolled to 20% thickness reduction. Isochronal annealing treatments were done from 300 to 1273 K in steps of 50 K in a vacuum of  $10^{-4}$  Pa. The annealing time for each temperature was fixed at 30 min. Isothermal annealing treatments were done at four different temperatures viz. 873, 923, 1073 and 1123 K from  $10^{-2}$  to  $10^3$  h in a vacuum of  $10^{-4}$  Pa. Positron lifetime measurements were carried out at room temperature after each isochronal and isothermal annealing step using a spectrometer having a time resolution of 225 ps (FWHM). The measured positron lifetime spectra were analysed into different lifetime components and their intensities using programmes RESOLUTION and POSITRONFIT [14].

## 3. Results and discussion

### 3.1. Isochronal annealing studies

Positron lifetime measurements were carried out on 20% cold worked (CW) D-9 alloy to monitor the defect recovery during isochronal annealing. Fig. 1 shows the variation of positron lifetime  $\tau$ , with annealing temperature for 20% CW sample. For comparison, the recovery curve corresponding to 17.5% CW D-9 [12] is also in-

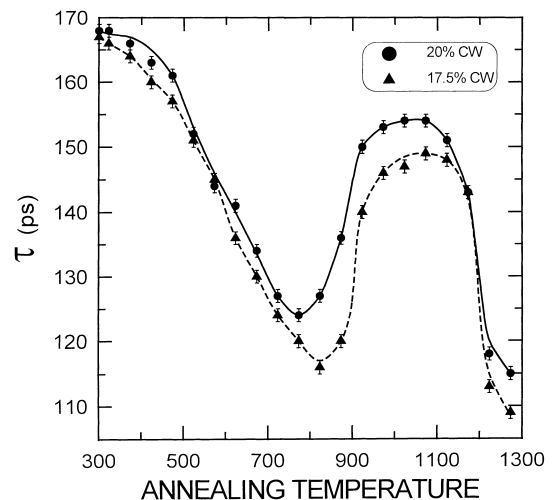


Fig. 1. Variation of positron lifetime with annealing temperature for D-9 alloy cold worked to 20% (solid circle) and 17.5% (solid triangles) thickness reduction. The data for 17.5% are taken from our earlier study [12].

cluded in Fig. 1. Only one lifetime component is resolved in the entire annealing range. Positron lifetime in the solution annealed state for D-9 alloy is  $110 \pm 1$  ps and that in the 20% CW sample is  $167 \pm 2$  ps which corresponds to saturation trapping of positrons at cold work induced defects [12]. The observed variation of lifetime  $\tau$  in Fig. 1 shows four distinct stages viz., (a) an initial monotonic decrease in  $\tau$  from CW state till 823 K, which corresponds to point defect recovery [12], (b) followed by a sharp increase in the interval 823–973 K, which corresponds to the formation of TiC precipitates, giving rise to positron trapping at misfit dislocations [12], (c) a plateau region in the interval of 973–1073 K, suggesting the completion of TiC precipitation and stability of these precipitates and (d) beyond 1073 K, a final decrease to near solution annealed state corresponding to the growth of TiC precipitates during recrystallisation [12].

The stage (a), corresponding to point defect recovery, is identified by comparing positron lifetime results on defect recovery in cold worked D-9 and in a model alloy without titanium [12]. The point defect recovery is seen to be identical in both cases. The stages (b)–(d), which occur beyond point defect recovery stage, are completely absent in model alloy without titanium [12] and hence, these three stages are associated with the presence of titanium in D-9 alloy. It is well established that TiC precipitates are formed above 800 K in Ti-stabilised stainless steels [4]. These precipitates have high lattice mismatch, which results in the generation of misfit dislocations [4]. These misfit dislocations form effective traps for positrons beyond the recovery of point defects. The stage (b), which shows an increase in positron lifetime,

corresponds to an increase in positron trapping rate. The increase in positron trapping rate can arise either due to a change in the nature of positron traps or due to increase in the number density of traps. Since the only traps for positrons are misfit dislocations at these temperatures, the increase in positron trapping rate is attributed to the increase in number density of misfit dislocations [12]. The increase in number density of misfit dislocations can only arise from increased concentration of TiC precipitates. Hence, the stage (b) is attributed to TiC precipitate formation [12]. The positron lifetime shows saturation value of  $\sim 152$  ps in stage (c). The saturation in lifetime in stage (c) implies completion of TiC precipitation [12]. The decrease in lifetime corresponding to stage (d) suggests that the number density of TiC precipitates is decreasing. Coarsening of TiC precipitates due to recrystallisation in this temperature regime was observed in Ti-stabilised stainless steel [4]. Hence, stage (d) is attributed to TiC precipitate coarsening during recrystallisation [12].

In the case of 20% CW D-9, TiC precipitate formation starts at a lower temperature as compared to 17.5% CW sample (Fig. 1). This is understandable as the higher degree of cold work provides larger density of dislocations which ultimately control TiC precipitation [15]. It is also interesting to note that the plateau value is higher for 20% CW sample as compared to 17.5% CW sample, implying that the number density of nucleated TiC precipitates is higher in the former sample. Hence, 20% cold work provides higher density of fine TiC precipitates as required by material design [1,2]. This finding again supports the choice of cold work level to be 20%, based on hardness measurements [6]. Though the lifetime behaviour above 1100 K, corresponding to the recrystallisation assisted growth of TiC precipitates, is alike for 17.5% and 20% CW samples, 20% CW sample seems to retain a small fraction of TiC precipitate structure as revealed by the slightly larger value of  $\tau$  even at 1273 K, as compared to the solution annealed value.

### 3.2. Isothermal annealing studies

In order to monitor the kinetics of formation and growth of TiC precipitates isothermal annealing studies were carried out at 873, 923, 1073 and 1123 K as a function of time from  $10^{-2}$  to  $10^3$  h. The above temperatures are so chosen that both nucleation and growth stages of TiC precipitates are covered. Fig. 2 shows the variation of positron lifetime as a function of annealing time for different temperatures. As seen from Fig. 2, the time evolution of the stages discussed in the previous section are observed in the isothermal annealing curves corresponding to 1073 and 1123 K. On the other hand, 873 and 923 K samples do not show the last stage corresponding to the recrystallisation assisted growth of

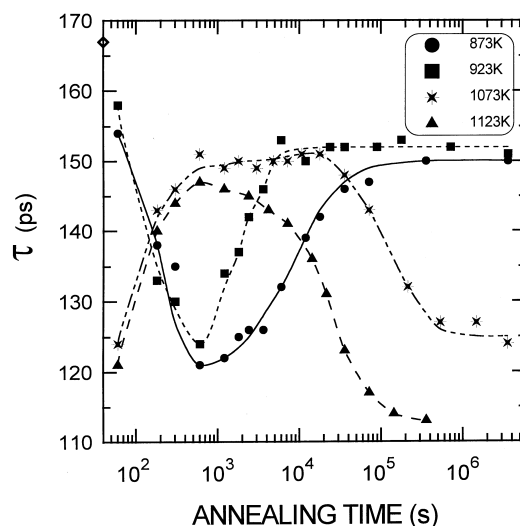


Fig. 2. Variation of positron lifetime as a function of isothermal annealing time for different annealing temperatures of 873, 923, 1073 and 1123 K. Lines are drawn to guide the eye. As-cold-worked value is shown in  $\tau$ -axis.

TiC precipitates. Stage (a), namely, point defect recovery, is seen to be complete in 10 min for 873 and 923 K, while it took just a minute for point defect recovery at 1073 and 1123 K. This is understandable, as these annealing temperatures are well above the point defect recovery stage seen in isochronal annealing studies shown in Fig. 1. It is interesting to note that the value of lifetime  $\tau$  after point defect recovery, is still higher than the defect free value for all temperatures. This is understood as due to the retention of significant dislocation density in the sample because of the nucleation of TiC precipitates on dislocations which arrest the movement of dislocations. The stage (b), which correspond to the formation of TiC precipitates, is marked by an increase in lifetime  $\tau$  towards a saturation value of  $\sim 152$  ps. The onset of this stage is seen to shift towards shorter times with increasing temperature. However, increasing the temperature beyond 1073 K does not show any change in stage (b). This implies that beyond 1073 K, the formation of TiC precipitates is not completely controlled by a thermally activated process. The plateau region (c) which signifies the stability of TiC precipitates [12], is seen to extend beyond 1000 h ( $10^6$  s) for 873 and 923 K. With increasing temperature, plateau region is found to narrow down. Finally, the region (d), corresponding to the TiC precipitate growth during recrystallisation [12], is not seen even up to 1000 h of annealing at 873 and 923 K. As the temperature is increased, the onset of recrystallisation shifts to shorter times which is the characteristic of a thermally activated process. It is interesting to note that the lifetime value reaches close to solution annealed state for 1123 K. On the other hand, for

1073 K sample, lifetime  $\tau$  tends to level off around 125 ps beyond 100 h ( $3 \times 10^5$  s). This implies that the TiC precipitate coarsening is not complete and considerable fraction of smaller TiC precipitates are still present. TEM results of Kesternich [15] clearly show the presence of TiC precipitates in Ti-stabilised stainless steel 1.4970 annealed at 1073 K.

Fig. 3 shows microstructures of D-9 alloy corresponding to: (a) solution annealed, (b) 20% cold worked, (c) cold worked and annealed at 923 K for 1000 h, (d) cold worked and annealed at 1073 K for 1000 h and

(e) cold worked and annealed at 1123 K for 100 h. Microstructure of solution annealed sample shows austenite grains of size  $\sim 20 \mu\text{m}$ , typical of well annealed state. Cold worked sample shows deformed grains with etch pits revealing dislocation structure. Microstructure of cold worked alloy annealed at 923 K for 1000 h (Fig. 3(c)) shows no recrystallisation and cold worked structure is retained even after this long annealing treatment. No TiC precipitates are seen in Fig. 3(c). For annealing at 1073 K for 1000 h, recrystallisation is seen to set-in and etched grain boundaries are not seen.

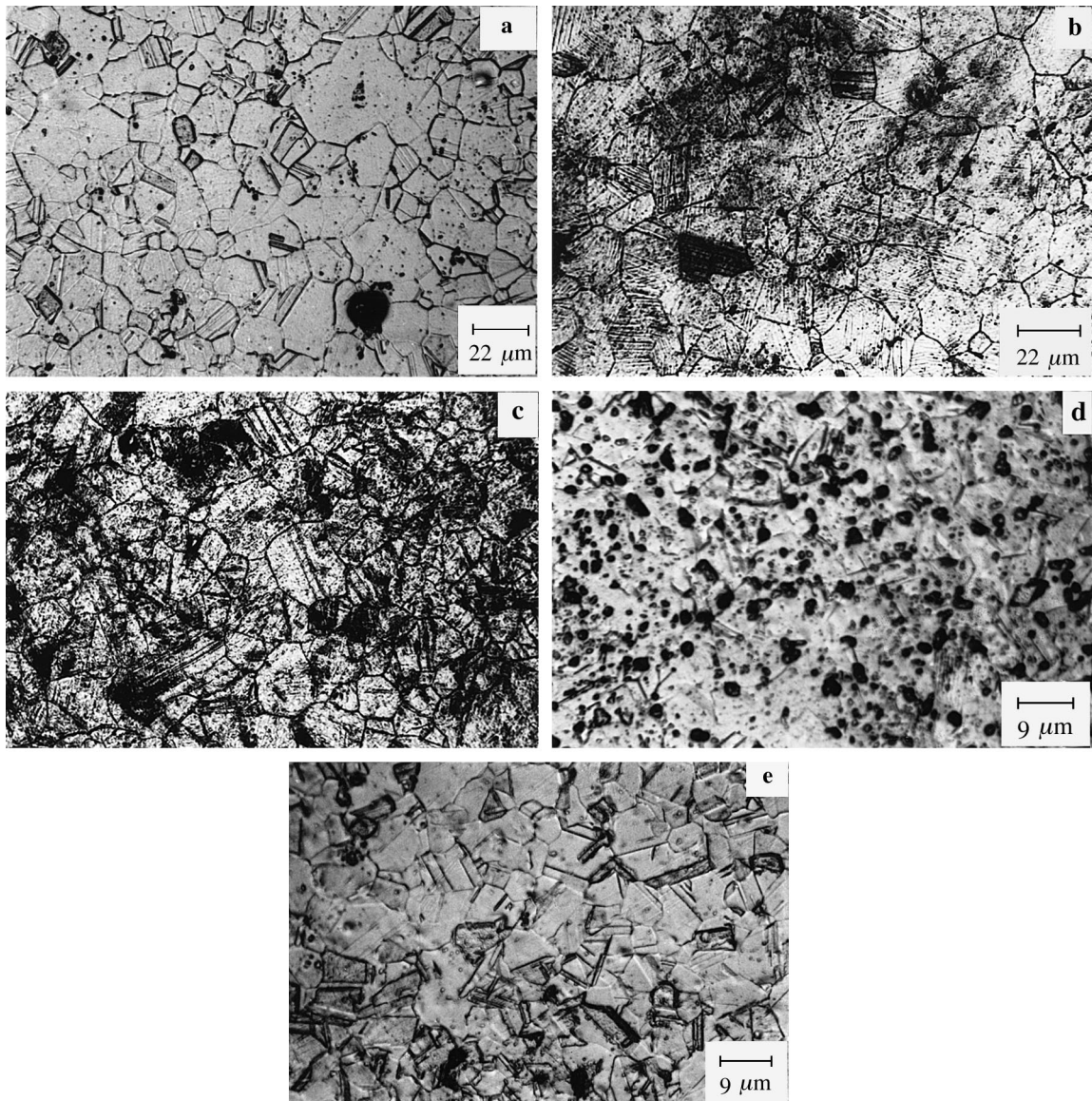


Fig. 3. Optical micrographs of D-9 alloy corresponding to different conditions of: (a) solution annealed, (b) 20% cold worked, (c) cold worked + annealed at 923 K for 1000 h, (d) cold worked + annealed at 1073 K for 1000 h and (e) cold worked + annealed at 1123 K for 100 h.

However, the microstructure of this sample exhibits a significant density of secondary TiC precipitates (Fig. 3(d)). On the other hand, annealing at 1123 K for 100 h results in recrystallised grains with very few TiC precipitates, as seen in Fig. 3(e).

### 3.2.1. TiC precipitate formation

TiC precipitates have large positive misfit of  $\sim 21\%$  in the austenitic matrix [15]. The possibility of relieving parts of the strain energy arising out of this large misfit, by replacement of section of the grain boundary or dislocations by the precipitate nuclei increases the probability of nucleation of TiC precipitates at edge dislocations and incoherent grainboundaries. Kesternich [15–17] reported extensive TEM studies on TiC precipitation in Ti-modified stainless steel and concluded that TiC precipitation require dislocations as nucleation centres. Indeed, our positron lifetime measurements on solution annealed D-9 sample subjected to isochronal treatment, do not show any TiC precipitation. This coupled with the fact that the cold worked sample shows TiC precipitation agrees well with the TEM observation of Kesternich [16].

Precipitate formation can be controlled by solute diffusion in the bulk, pipe diffusion through dislocations, interfacial reactions at precipitate-matrix boundaries and mutual dislocation recovery along with precipitate formation [16]. As seen from Fig. 2, the stage (b) corresponding to increase in average lifetime is attributed to TiC precipitate formation [18]. This increase in average lifetime is brought about by the increase in the number density of TiC precipitates. This precipitation stage is a thermally activated process as seen from Fig. 2, where increase in temperature decreases the time for precipitate formation. However, the subsequent saturation in lifetime after a certain annealing time indicates that the precipitate formation is complete and that the coarsening of so-formed precipitates is retarded. It should be noted that beyond 1073 K, the saturation behaviour of lifetime changes. Also, the plateau region for 1123 K is less prominent. This aspect may be attributed to recrystallisation induced precipitate coarsening which is discussed in Section 3.2.2.

In order to study the kinetics of TiC precipitate formation below 1073 K, a nucleation parameter is defined as  $\{(\tau - \tau_b)/(\tau_{ppt} - \tau_b)\} \times 100$ , where,  $\tau_b$  is lifetime of defect free sample and  $\tau_{ppt}$  is the saturation lifetime at misfit dislocations associated with TiC precipitates. The above expression for the nucleation parameter has the following implications. Any increase in average lifetime  $\tau$  can arise either from a change in the nature of defect that trap positrons or increase in the defect concentration [9]. For the high annealing temperatures above point defect recovery in the present study, the only trap for positrons is the misfit dislocation associated with the TiC precipitates. Thus ruling out any change in the

nature of defect responsible for lifetime variation, the observed increase in  $\tau$  beyond a certain annealing time, signifies the increase in the concentration of TiC precipitates. Hence, the nucleation parameter, as defined above, is a measure of the percentage increase in the concentration of so-formed TiC precipitates. Fig. 4 shows variation of nucleation parameter as a function of annealing time for 873, 923 and 1073 K. A horizontal line is drawn corresponding to 50% increase in nucleation parameter. For the limited temperature regime under consideration, an apparent activation energy of 1.6 eV is estimated. This rules out Ti diffusion in austenitic matrix as the rate limiting process, since it requires a much higher activation energy of 2.6 eV [19]. Considering the non-equilibrium nature of the TiC precipitate formation process, a more detailed modelling of precipitate nucleation kinetics such as the one developed for Nb(CN) precipitates in austenitic steels [20] is needed for further understanding. However, such an analysis is beyond the scope of this paper.

### 3.2.2. Recrystallisation assisted precipitate coarsening

It is seen from Fig. 2 that positron lifetime continues to be at the saturation value even after 1000 h of annealing at 873 and 923 K. However at higher temperature range  $\geq 1073$  K, positron lifetime shows a systematic decrease to a new value which is still larger than that of bulk austenite. This decrease is associated with TiC precipitate coarsening during recrystallisation at higher temperatures [18]. Such a behaviour has also been reported from hardness studies in D-9 [21,22]. It is clear that recrystallisation sets in at earlier times for higher annealing temperatures, as can be seen from the fact that

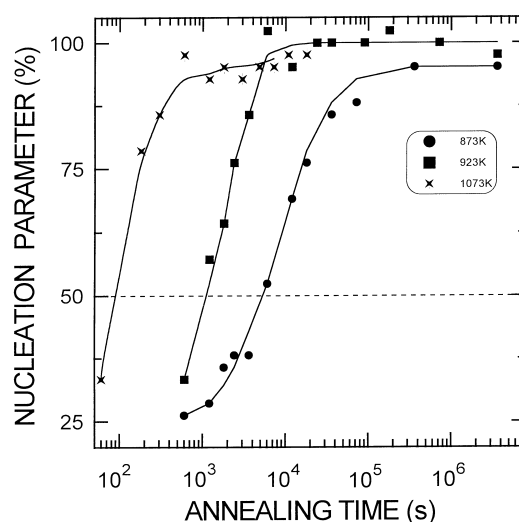


Fig. 4. Variation of nucleation parameter (see text) with annealing time for 873, 923 and 1073 K. Dashed horizontal line shows 50% nucleation level for TiC precipitates.

the plateau region corresponding to saturation lifetime  $\tau$  is less pronounced for the case of 1123 K anneal, as compared to that for 1073 K anneal (Fig. 2). A growth parameter, similar to the nucleation parameter discussed in previous section, is defined as  $\{(\tau_{\text{ppt}} - \tau)/(\tau_{\text{ppt}} - \tau_b)\} \times 100$ . This parameter which has the same implication as that discussed in Section 3.2.1, is a measure of the percentage change in TiC precipitate concentration due to coarsening. Fig. 5 shows variation of growth parameter as a function of annealing time for 923, 1073 and 1123 K. As seen from Fig. 5, the precipitate growth is temperature dependent, showing a decrease in time for 50% growth with increasing annealing temperature. Unfortunately, among the temperatures chosen in the present study, only 1073 and 1123 K show the growth behaviour which restricts the computation of activation energy for recrystallisation controlled growth of TiC precipitates.

#### 4. Conclusions

The formation and growth of TiC precipitates in D-9 alloy has been studied by positron lifetime spectroscopy. Since TiC precipitates have large positive misfit in the austenitic matrix, positron trapping at misfit dislocations has been used as a signature to monitor the kinetics of formation and growth of TiC precipitates. TiC precipitates are found to be more stable for 20% cold working than 17.5%. From the isothermal annealing studies, it is found that TiC precipitation is controlled by dislocations. A limited temperature dependency of dislocation controlled TiC precipitation is observed with an

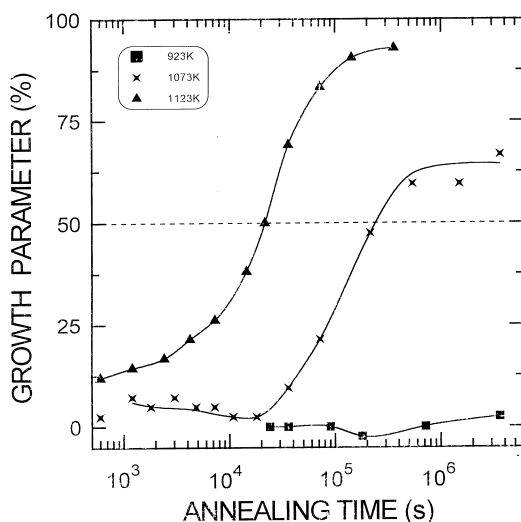


Fig. 5. Variation of growth parameter (see text) as a function of annealing time for 923, 1073 and 1123 K. Dashed horizontal line marks the completion of 50% of growth of TiC precipitates.

apparent activation energy of 1.6 eV in 20% cold worked D-9 alloy. TiC precipitates are found to be stable against growth even after 1000 h of annealing at  $\leq 923$  K. For higher annealing temperatures  $\geq 1073$  K, the observed growth curves indicate strong recrystallisation assisted TiC precipitate coarsening. Since TiC precipitates are efficient traps for helium and vacancies, the present results may be significant in the context of evaluation of helium embrittlement and void swelling in the D-9 alloy.

#### Acknowledgements

The authors gratefully acknowledge Shri. V. Madhurai Muthu for his help in metallographic observations.

#### References

- [1] L.K. Mansur, E.H. Lee, P.J. Maziasz, A.P. Rowcliffe, *J. Nucl. Mater.* 141 (1986) 633.
- [2] W. Kesternich, *J. Nucl. Mater.* 127 (1985) 153.
- [3] S. Venkadesan, A.K. Bhaduri, P. Rodriguez, K.A. Padmanabhan, *J. Nucl. Mater.* 186 (1992) 177.
- [4] W. Kesternich, D. Meertens, *Acta Metall.* 34 (1986) 1071.
- [5] K. Herschback, W. Schneider, K. Ehrlich, *J. Nucl. Mater.* 203 (1993) 233.
- [6] M. Vasudevan, S. Venkadesan, P.V. Sivaprasad, S.L. Mannan, *J. Nucl. Mater.* 211 (1994) 251.
- [7] H.R. Brager, *J. Nucl. Mater.* 57 (1975) 103.
- [8] J.L. Straalsund, H.R. Brager, *Trans. ANS* 15 (1972) 251.
- [9] K. Peterson, in: W. Brandt, A. Dupasquier (Eds.), *Positron Solid State Physics*, North-Holland, Amsterdam, 1983, p. 298.
- [10] A. Bharathi, C.S. Sundar, *Mater. Sci. Forum* 105 (1992) 905.
- [11] B. Viswanathan, G. Amarendra, R. Rajaraman, in: R.E. Stoller, A.S. Kumar, D.S. Gelles (Eds.), *Proceedings of the 15th International Symposium ASTM-STP1125*, ASTM, Philadelphia, 1992, p. 495.
- [12] R. Rajaraman, P. Gopalan, B. Viswanathan, S. Venkadesan, *J. Nucl. Mater.* 217 (1994) 325.
- [13] S. Venkadesan, P.V. Sivaprasad, M. Vasudevan, S. Venugopal, P. Rodriguez, *Trans. Ind. Inst. Met.* 45 (1992) 57.
- [14] P. Kirkegaard, M. Eldrup, O.E. Mogensen, N.J. Pedersen, *Comput. Phys. Commun.* 68 (1981) 307.
- [15] W. Kesternich, *Radiat. Eff.* 78 (1983) 261.
- [16] W. Kesternich, *Philos. Mag.* A 52 (1985) 533.
- [17] W. Kesternich, *J. Nucl. Mater.* 155–157 (1988) 1025.
- [18] P. Gopalan, R. Rajaraman, B. Viswanathan, K.P. Gopinathan, S. Venkadesan, *Solid State Phys. (India)* 38C (1995) 213.
- [19] E.A. Brandes, G.B. Brook, (Eds.), *Smithells Metals Reference Book*, 7th ed., Butterworths, Oxford, 1992, p. 13–84.
- [20] W.J. Liu, *Metall. Mater. Trans.* 26A (1995) 1641.
- [21] M. Vasudevan, S. Venkadesan, P.V. Sivaprasad, *J. Nucl. Mater.* 231 (1996) 231.
- [22] M. Vasudevan, S. Venkadesan, P.V. Sivaprasad, *Mater. Sci. Technol.* 12 (1996) 338.